

# Tissue-Engineered Small Intestine Improves Recovery After Massive Small Bowel Resection

Tracy C. Grikscheit, MD,\*‡ Aleem Siddique, BA,\*‡ Erin R. Ochoa, MD,†‡ Ashok Srinivasan, PhD,§ Eben Alsberg, PhD,|| Richard A. Hodin, MD,\*‡ and Joseph P. Vacanti, MD\*‡

**Objective:** Rescue with tissue-engineered small intestine (TESI) after massive small bowel resection (MSBR).

**Summary Background Data:** Short bowel syndrome is a morbid product of massive small bowel resection. We report the first replacement of a vital organ by tissue engineering with TESI after MSBR.

**Methods:** Ten male Lewis rats underwent TESI implantation with green fluorescent protein (GFP)-marked cells (TESI+, n = 5) or sham laparotomy (TESI-, n = 5) followed by MSBR. Side-to-side anastomosis of TESI to proximal small intestine was performed or omitted. TESI∅ animals underwent implantation of engineered intestine with no further surgery. Weights were measured QOD until day 40. Transit times were measured. DNA assay was performed with computer morphometry. Northern blots of RNA were probed for intestinal alkaline phosphatase (IAP) and villin. Hematoxylin and eosin, S100, and smooth muscle actin immunohistochemistry were performed. Blood was collected at sacrifice.

**Results:** All 10 rats initially lost then regained weight. The initial rate of weight loss was higher in TESI+ versus TESI-, but the nadir was reached a week earlier with more rapid weight gain subsequently to 98% preoperative weight on day 40 in animals with engineered intestine versus 76% ( $P < 0.03$ ). Serum B12 was higher at 439 pg/mL versus 195.4 pg/mL. IAP mRNA appeared greater in TESI+ than TESI∅, with constant villin levels. Histology revealed appropriate architecture including nerve. GFP labeling persisted.

**Conclusions:** Anastomosis of TESI significantly improved postoperative weight and B12 absorption after MSBR. IAP, a marker of

differentiation in intestinal epithelium, is present in TESI, and GFP labeling was accomplished.

(*Ann Surg* 2004;240: 748–754)

Short bowel syndrome (SBS) includes a broad diversity of metabolic and physiologic disturbances, including fluid, nutrient, and weight loss secondary to unavailable functional surface area.<sup>1</sup> Calcium, magnesium, zinc, iron, B12, and fat-soluble vitamin deficiencies are complicated by decreased absorption of carbohydrates and protein, which are linked as well to metabolic acidosis, formation of biliary and renal calculi, dehydration, and weight loss.<sup>2</sup> SBS generally occurs with loss of approximately 70% to 75% of the small intestine.<sup>3–5</sup> The severity of SBS is linked to the extent of resection, presence of an ileocecal valve, and presence of jejunum,<sup>2</sup> as well as the health of the remaining small bowel.<sup>4</sup>

Our laboratory first reported making tissue-engineered small intestine (TESI) by the transplantation of organoid units on a polymer scaffold into the omentum of the Lewis rat.<sup>6</sup> Organoid units are multicellular units derived from neonatal rat intestine, containing a mesenchymal core surrounded by a polarized intestinal epithelium, and contain all of the cells of a full-thickness intestinal section.<sup>7</sup>

We have recently transformed this protocol to yield significantly more organoid units in a shorter time from more specific areas of the gastrointestinal tract, beginning with the sigmoid colon as reported in this journal,<sup>8</sup> leading to a greater viability, as production of tissue-engineered colon (TEC) occurs 100% of the time from autologous tissue, syngeneic tissue, or TEC itself. We have generated specific areas of the entire gastrointestinal tract including the abdominal esophagus,<sup>9</sup> stomach,<sup>10</sup> gastroesophageal junction,<sup>10</sup> ileum and jejunum, and portions of the colon (Fig. 1). The sigmoid colon alone, harvested and grown into TEC and used in a replacement model, demonstrates resilient architecture, sodium and water absorption, short-chain fatty acid production, and ganglion cells.<sup>11</sup> In the case of TEC, the model in which much of the protocol refinement was done, the histology has improved

From the \*Department of Surgery and †Department of Pathology, Massachusetts General Hospital, Boston, Massachusetts; ‡Harvard Medical School, Center for the Integration of Medicine and Innovation in Technology, Boston, Massachusetts; §Cardiovascular Research Center, Massachusetts General Hospital, Boston, Massachusetts; and the ||Department of Chemical Engineering, University of Michigan, Ann Arbor, Michigan. Funding from the Center for the Integration of Medicine and Innovation in Technology, Department of Defense DAMDIT-99-2-9001.

Reprints: Joseph P. Vacanti, MD, Department of Pediatric Surgery, Massachusetts General Hospital, Warren 1157, 55 Fruit Street, Boston, MA 02114. E-mail: jvacanti@partners.org.

Copyright © 2004 by Lippincott Williams & Wilkins

ISSN: 0003-4932/04/24005-0748

DOI: 10.1097/01.sla.0000143246.07277.73

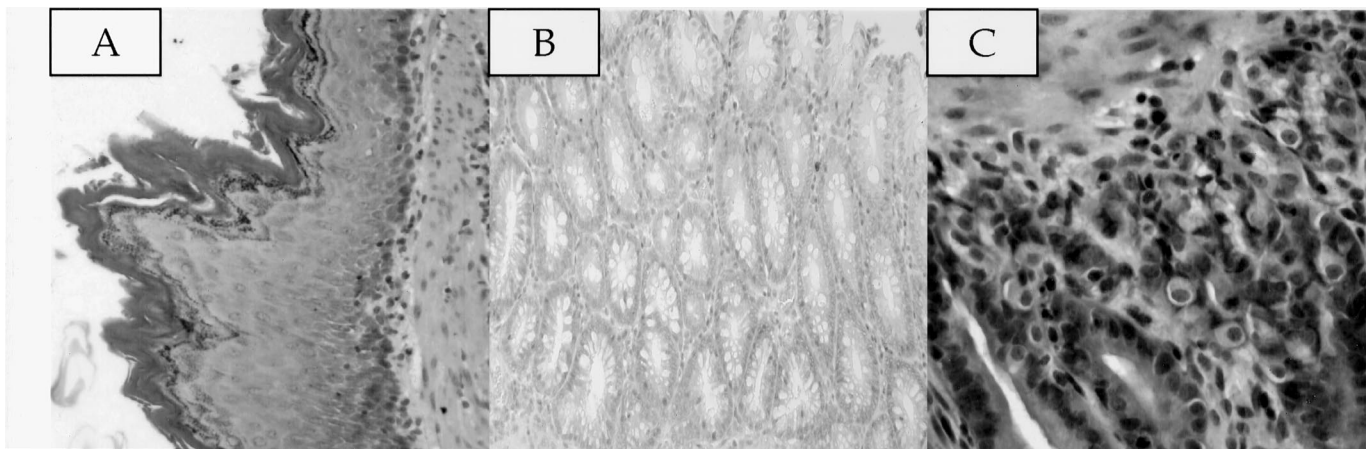


**FIGURE 1.** A, Tissue engineered esophagus, original magnification  $20\times$ . B, Tissue engineered colon, original magnification  $20\times$ . C, Tissue engineered stomach; note large lucent parietal cells and glandular structure, original magnification  $20\times$ . All tissues engineered in the Lewis rat model.

to be indistinguishable in some cases from native colon with an appropriate epithelial layer, actin-positive muscularis propria containing S100-positive cells in the distribution of Meissner and Auerbach's plexi, as well as lucent adjacent ganglion cells.<sup>8</sup>

Preliminary data showed that TESI generated by our new protocol has markedly improved tissue architecture, including a mucosal immune system with an immunocyte population similar to that of native small intestine.<sup>12,13</sup> In addition, response of TESI to exogenous GLP-2 includes mucosal growth and enhanced SGLT1 expression.<sup>14</sup>

We hypothesized that together these findings indicated TESI could aid in recovery of SBS. In addition, we sought to confirm the correct architecture of TESI seen on initial histology by performing computer morphometry and immunohistochemistry to assess for nerve and muscle components. To prove the donor origin of the TESI, we sought to label the progenitor cells with green fluorescent protein (GFP), which has additional implications for future more useful transfections, and we initiated confirmation of the differentiated state of the enterocytes in TESI after anastomosis by studying the villin and intestinal alkaline phosphatase content by Northern blot.

## MATERIALS AND METHODS

### Generation of Organoid Units

Small intestine organoid units were produced by dissecting the small intestine without mesentery from 6-day-old Lewis rat pups ( $n = 40$ ), once lumenally irrigated with cold Hanks' balanced salt solution (HBSS), then cut into full thickness 2-mm  $\times$  2-mm sections after lengthwise opening along the antimesenteric border. TESI was isolated from nonspecific areas of small intestine, with care to avoid including duodenum or very terminal ileum, but including both

ileum and jejunum. These were washed twice in  $4^{\circ}\text{C}$  HBSS, sedimenting between washes, and digested with dispase 0.25 mg/mL and collagenase 800 U/mL on an orbital shaker at  $37^{\circ}\text{C}$  for 25 minutes. The digestion was immediately stopped with 3  $4^{\circ}\text{C}$  washes of a solution of high glucose Dulbecco Modified Eagle Medium (DMEM), 4% heat-inactivated fetal bovine serum (iFBS), and 4% sorbitol. The organoid units were centrifuged between washes at  $150\times g$  for 5 minutes, and the supernatant removed. Organoid units were reconstituted in high-glucose DMEM with 10% iFBS, counted by hemocytometer, transfected with GFP as described below, and loaded 100,000 units per polymer at  $4^{\circ}\text{C}$ . Constructs were maintained at that temperature until implantation, which occurred in under 1.5 hours.

### GFP Signal Production

GFP-labeled OU underwent incubation with the GFP-VZV virus at an MOI of 10 at  $37^{\circ}\text{C}$  on an orbital shaker for 1.5 hours; 200,000 OU were maintained in a 12-well plate to measure GFP production in vitro in 24 hours to confirm virus activity, and the remaining OU were implanted. Production of GFP was performed as follows. A MoMLV (Moloney murine leukemia virus) retroviral vector with GFP expressed from an endogenous CMV promoter was used. The virus was pseudotyped with the VSV (vesicular stomatitis virus) glycoprotein to allow efficient infection of the rat organoids. Virus was produced following transient transfection in 293-GPG cells. This retroviral producer cell line provides the retroviral packaging functions in trans and allows expression of the VSV-G protein in a tetracycline-regulatable fashion.<sup>15</sup> Seventy-five dishes were transfected with the retroviral vector DNA (10  $\mu\text{g}$ ) in the absence of tetracycline, using Lipofectamine (Invitrogen). The medium was changed every 24

hours. Tissue-culture supernatants containing virus were harvested every 24 hours at the 72-, 96-, 120-, and 144-hour time points. Harvested supernatants were clarified by low-speed centrifugation. The viral supernatants were then filtered through a 0.45- $\mu$ m filter and immediately concentrated up to a 1000-fold by centrifugation at 17,000 RPM, 4°C. The resulting pellets containing concentrated virus were resuspended in buffer containing 8  $\mu$ g/mL polybrene (Sigma H 9268) at 4°C overnight and pooled. Titers were estimated using the GFP signal following infection of 293 cells. GFP detection 2 weeks after anastomosis was performed on 10- $\mu$ m frozen section and with native tissue controls.

### TESI Implantation

Scaffold polymers were constructed of 2-mm-thick nonwoven polyglycolic acid (Smith and Nephew, Heslington, NY), formed into 1-cm tubes (outside diameter = 0.5 cm, inside diameter = 0.2 cm), and sealed with 5% poly-L-lactic acid (Sigma-Aldrich, St. Louis, MO). Polymer tubes were sterilized in 100% ethanol at room temperature for 20 minutes, then washed with 500 mL of phosphate-buffered saline (PBS), coated with 1:100 collagen type 1: PBS solution for 20 minutes at 4°C, and washed again with 500 mL PBS. Polymer tubes were internally loaded with organoid units by micropipette.

Under pentobarbital anesthesia, 5 150-g male Lewis rats were implanted with TESI (group TESI+). Implantation was achieved through a 1.5-cm upper abdominal incision, through which the greater omentum was externalized and wrapped in a specific manner around the TESI construct, secured with a 6-0 Prolene suture, and returned to the peritoneum before closing the abdomen in layers. Five rats from the same cohort underwent sham laparotomy with no TESI implantation (group TESI-). A third group, TESI $\emptyset$ , underwent implantation analogous to group TESI+, with no further surgery. TESI- and TESI+ groups were compared, and each was composed of 5 animals each. TESI $\emptyset$  animals did not undergo bowel resection. TESI $\emptyset$  animals were used only for the purpose of RNA analysis as an example of the tissue engineered intestine RNA content immediately after TESI development.

### Massive Small Bowel Resection and Rescue Anastomosis

Four weeks later, massive small bowel resection was performed in TESI+ and TESI- animals with end-to-end anastomosis 5 cm distal to duodenum and 5 cm proximal to cecum, comprising a greater than 80% resection. Measurements of small intestine in 8 animals from the same cohort had been completed prior to resection, with an average bowel length of 72 cm, and standardized resections were guaranteed by checking both lengths and consistent resection in relationship to the vascular arcades. Side-to-side anastomosis of

TESI to proximal small intestine was performed (TESI+) or omitted (TESI-). Animals were housed in the Animal Research Facility of the Massachusetts General Hospital, Boston, MA, in accordance with the National Institutes of Health guidelines for care of laboratory animals, and pair-fed throughout the experiment. Animals were pair-fed, matching TESI-/TESI+ animals by their chronologic role in TESI creation or anastomosis (first, second, etc). Intake of rat chow in grams was not statistically significantly different between pairs.

### Data Collection and Histology

Weights were measured QOD until day 40 sacrifice, analyzed by 2-stage analysis or Mann-Whitney. Transit times were measured by red-dye gavage and 30-minute observation points. DNA assay was performed using standard protocol with Hoechst dye (H33258) after proteinase K digestion and standardization to calf thymus DNA stock solution and reported after unpaired *t* test with Welch correction. Computer morphometry compared villus heights, widths, and crypt and muscularis widths by a standardized morphometric computer program (Metamorph) and unpaired *t* test with Welch correction. Hematoxylin and eosin and smooth muscle actin immunohistochemistry were performed. Blood was collected after 12-hour fast at sacrifice for metabolic profile and measurement of B12 and gastrin level by the hospital's clinical laboratory. Immunohistochemistry was performed using the DAKO Envision kit to detect antigens monoclonal  $\alpha$  anti-smooth muscle actin (Sigma) and the S100 protein (DAKO). TESI and native bowel widths and lengths were measured at the time of anastomosis and at sacrifice. Bowel width was measured from the antimesenteric border to the mesenteric border with a caliper. Length of native intestine was measured in vivo with a 2-0 silk laid along the antimesenteric border, then measuring the silk, and compared with an in vivo measurement taken after anastomosis. The TESI was measured in the x, y, and z axes preanastomosis and at sacrifice. Width and length data was analyzed by Kruskal-Wallis.

### RNA Analysis

Rats that had not undergone any procedure were killed to obtain control RNA from segments of duodenum (pylorus to ligament of Treitz), jejunum (10 cm beginning at the ligament of Treitz and running distally), and ileum (10 cm beginning at the ileocecal valve and running proximally). RNA was extracted from the TESI in TESI+ rats and also from the TESI of rats in TESI $\emptyset$ . On the day of RNA extraction, the animals were killed by CO<sub>2</sub> inhalation overdose. Total RNA was extracted using the RNeasy-protect maxi kit (Qiagen, Valencia, CA) according to the manufacturer's protocol. For Northern blot analyses, 15  $\mu$ g of total RNA was combined with the appropriate amount of glyoxal loading dye (Ambion, Austin, TX), and the samples were

electrophoresed through agarose gels prepared in Northern-Max Gly Gel-Prep/Running Buffer (Ambion). Loading was determined by examination of ethidium bromide-stained gels and by probing for the actin transcript. After electrophoresis, the RNA was transferred onto positively charged nylon membranes (Amersham Pharmacia Biotech, Buckinghamshire, UK) and cross-linked in a Stratalinker 1880 UV hybridization oven (Stratagene, La Jolla, CA) at the auto-crosslink setting according to the manufacturer's protocol. Complementary DNA probes were  $^{32}\text{P}$ -radiolabeled to a specific activity of  $\sim 5 \times 10^8$  cpm/ $\mu\text{g}$  DNA. The intestinal alkaline phosphatase (IAP) probe is a 1.7-kb *Pst*I fragment derived from the human IAP cDNA and was obtained from ATCC (Rockville, MD).<sup>16</sup> The villin probe is a 530 bp *Sall*/*Bam*H I fragment from the human cDNA.<sup>17</sup> The actin probe is a 1.0-kb *Pst*I fragment derived from the mouse  $\beta$ -actin cDNA.<sup>18</sup> Hybridizations were carried out using the Rapid-hyb solution from Amersham Pharmacia Biotech at 65°C overnight. The membranes were then washed for 30 minutes twice at 65°C in a low stringency wash solution ( $2 \times \text{SSC}/0.1\%$  SDS) followed by a high-stringency wash ( $0.1 \times \text{SSC}/0.1\%$  SDS) at 65°C for 30 minutes after which they were subjected to autoradiography.

## RESULTS

All animals survived implantation and 100% of the TESI+ cohort generated TESI, oblate spheroidal cysts approximately  $3 \times 5 \times 4$  cm in the x, y, and z axes (Fig. 2). Histology revealed well-formed TESI positive for actin in the muscularis mucosa (Fig. 3), with ganglion cells appropriately

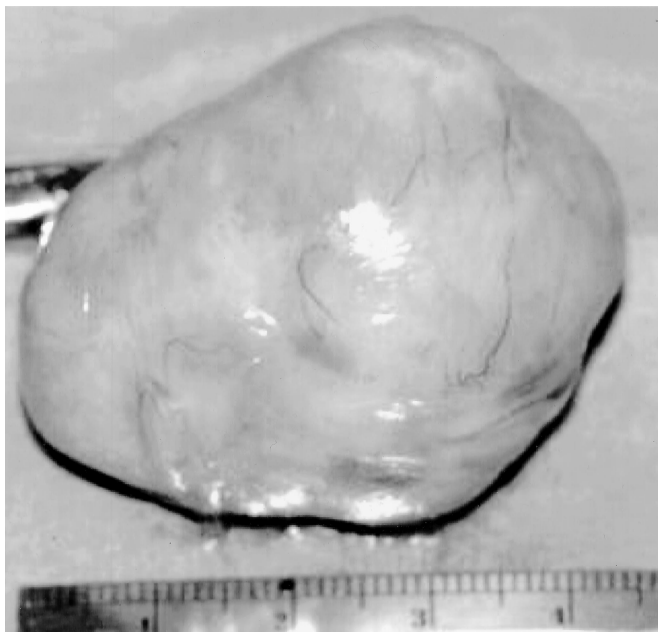


**FIGURE 2.** Gross appearance of a representative TESI cyst, 4 weeks after implantation in the omentum.

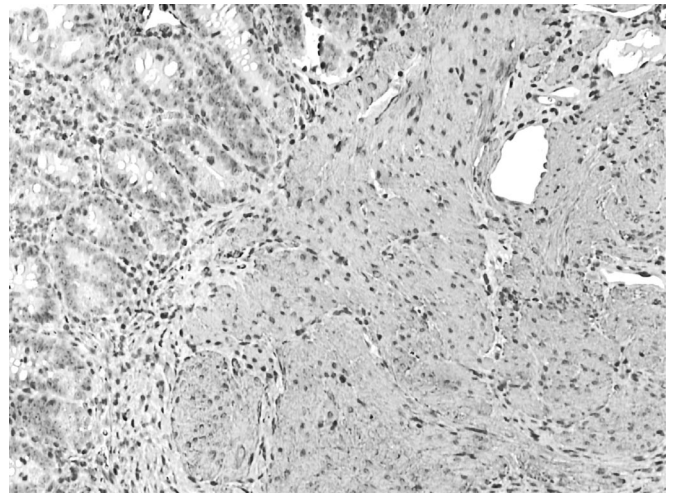


**FIGURE 3.** Immunohistochemical detection of the antigen smooth muscle actin is seen in the muscularis mucosa of the TESI 42 days after proximal anastomosis following massive small bowel resection,  $10 \times$ .

distributed in the locales of Auerbach and Meissner's plexi (Figs. 4 and 5). Epithelial development was not significantly different between TESI (Fig. 6) and native small intestine, with median villus heights of 239 and 272  $\mu$ , respectively ( $P = 0.1584$ ), median villus widths of 58 (TESI) and 52 (native)  $\mu$  ( $P = 0.1113$ ), median crypt widths of 20 (TESI) and 27 (TESI)  $\mu$  ( $P = 0.6362$ ). Width of the muscularis mucosa was greater in TESI (488  $\mu$ ) than in native SI (323  $\mu$ ) from the resected animals ( $P = 0.003$ ). DNA levels in ng/mg

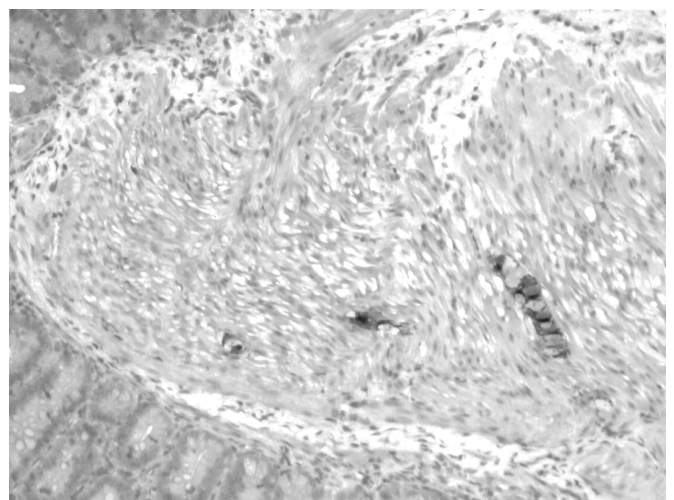


**FIGURE 4.** Immunohistochemical detection of the antigen S100 revealing plexi in TESI 42 days after proximal anastomosis following massive small bowel resection, original magnification  $10 \times$ . Lucent ganglion cells are seen central to the S100-positive cells.

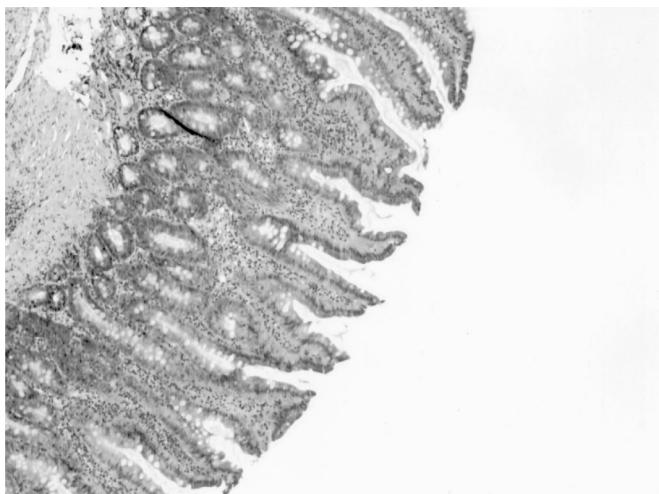


**FIGURE 6.** Hematoxylin and eosin stain, TESI, original magnification 10 ×.

dry weight were significantly elevated in the TESI in TESI+ animals ( $5778.4 \pm 3102$ ) compared with the native small intestine in TESI- animals ( $2547.5 \pm 1322$ ,  $P = 0.0365$ ).

There was no statistically significant change in the measurements of the anastomosed TESI segments. There was an increase in width by approximately 2 mm in the native bowel in both TESI+ and TESI- animals. There was no statistically significant difference in the increased bowel width between TESI+ and TESI- groups. There was no statistically significant increase in measured length of the native bowel segments.

All animals initially lost weight and then regained weight; however, animals with TESI reached their nadir at 7.7 days and then began to regain weight up to 98.5% of their

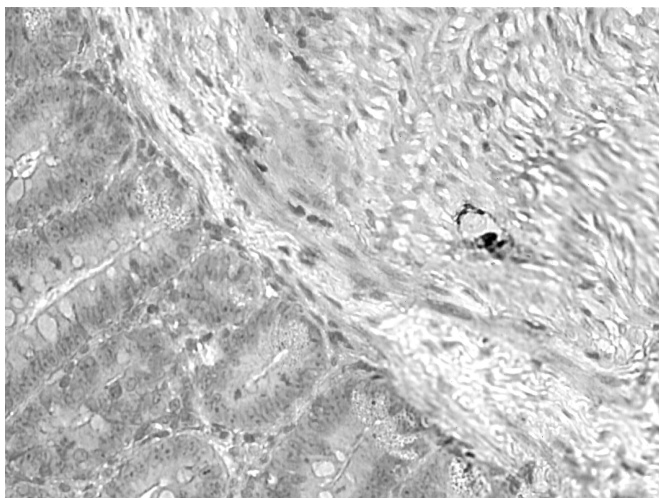


**FIGURE 5.** 20 × view of lucent ganglion cell central to the S100-positive cells seen in Figure 4 (same field).

preoperative weight by day 40, while TESI- animals lost weight for 14.6 days ( $P = 0.009$ ) and only regained back to 76.8% of their preoperative weight by day 40 ( $P < 0.03$ , Fig. 7). The animals in TESI- lost weight more rapidly for the first week ( $-3.1\%/d$  versus  $-1.8\%/d$ ,  $P = 0.068$ ) but because they lost weight for about half the amount of time the TESI- animals lost weight, their nadir was higher (78.9% TESI+ versus 72.1% TESI-,  $P = 0.05$ ). TESI+ animals regained weight more rapidly (0.7% preoperative weight/d regained) than TESI- animals (0.2%/d,  $P = 0.004$ ) after each group reached its nadir (Fig. 7).

There were no differences in metabolic serum profiles, fasting serum gastrin, or hematocrit between the 2 groups. Gastrin levels were elevated above 200 in 2 TESI- animals, with mean fasting gastrin of 109 (TESI+) versus 178.2 (TESI-), but this difference did not reach statistical significance ( $P = 0.1005$ ). Serum B12 was normal range in TESI+ animals (439 pg/mL) and deficient in TESI- animals (195.4 pg/mL,  $P = 0.0159$ ).

Transit times were significantly longer in animals with TESI (1825 minutes  $\pm$  753) than without (982  $\pm$  300,  $P = 0.0488$ ).

GFP labeling was detected in OU cultured for 24 hours and then in the TESI tissue at harvest on frozen section (Figs. 8 and 9). Adjacent native small intestine sections did not fluoresce.

Figure 10 shows the results of northern blots of RNA probed for IAP, villin, and actin. Both IAP and villin were detected in the TESI, indicating that the tissue had attained a

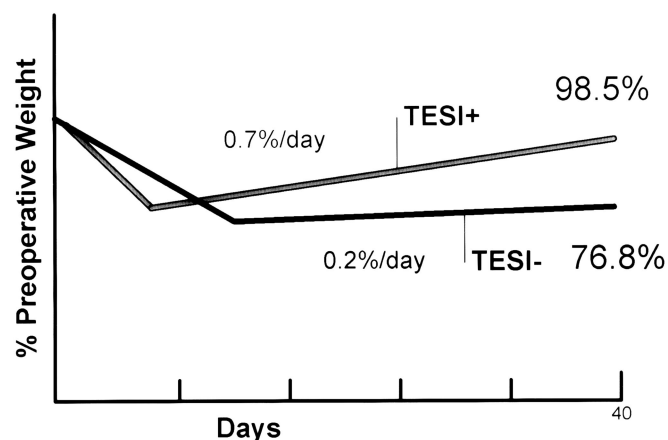


**FIGURE 7.** Preoperative Weight (%) for TESI+ and TESI- rats over 40 days. TESI+ animals reach their nadir at 7.7 days, while animals without TESI lose weight for an additional week. TESI+ animals regain weight to a higher percentage (98.5%) than TESI- animals (76.8%) by day 40. TESI+ animals regained weight more rapidly (0.7% preoperative weight/d regained) than TESI- animals (0.2%/d,  $P = 0.004$ ) after each group reached its nadir.

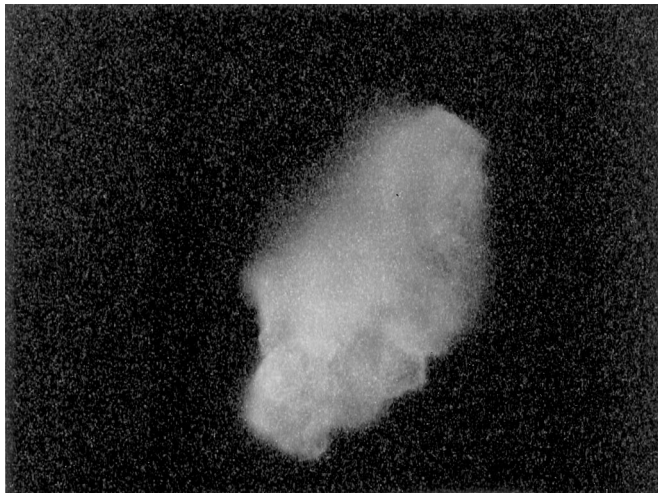


FIGURE 8. TESI OU labeled with GFP, 10 ×.

villus-like differentiated phenotype. As expected, the highest levels of IAP expression occurred in the duodenum and diminished significantly in the more distal segments. The level of IAP mRNA in the TESI from TESI+ rats appears greater than in the TESI in rats where it was left implanted in the greater omentum (TESI∅). The levels of villin mRNA were fairly constant along the length of the small intestine and appear similar in the TESI from the TESI+ rats and TESI∅ rats. Finally, the levels of actin demonstrate the loading of RNA in all lanes.

### DISCUSSION

The underlying principle of tissue engineering is exact replacement of tissue function and architecture that have been removed rather than replacement by proxy. In this case, we report TESI that is produced in a reasonable quantity with

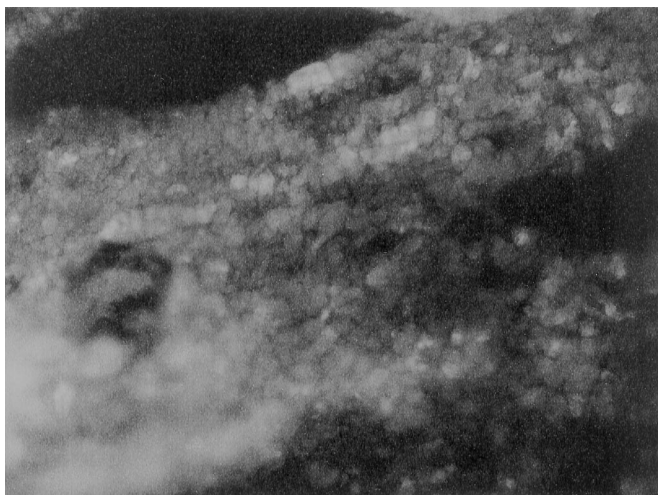


FIGURE 9. TESI labeled with GFP on harvest, 10 ×.

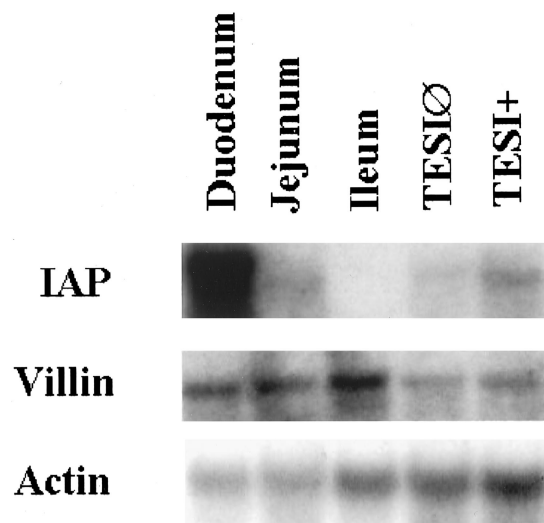


FIGURE 10. Representative Northern blot autoradiographs of total RNA from duodenum, jejunum, ileum, TESI from TESI+ rats, and TESI from TESI∅ rats. The RNA was probed for IAP and villin. Actin is included in the lower panel to demonstrate the loading of the RNA.

high efficiency. The histology with adjunct immunohistochemical studies of this novel tissue reflects intact epithelial, muscular, vascular, and neural components. This is the first demonstration of ganglion cells and S-100-positive groupings in TESI. In addition, this is the first report of a tissue-engineered vital organ functioning as a salvage therapy in a replacement model. It was physiologically advantageous for animals after massive bowel resection to have an attached segment of TESI, reducing the overall period of weight loss by half (7.7 versus 14.6 days) and maintaining and then regaining higher percentages of weight than those animals who had massive small bowel resection alone. Animals with TESI had nearly returned to their preoperative weight at 40 days (98.5%) while those without were significantly less recovered (76.8%). Transit times were longer in TESI+ animals. Possible evidence of superior absorptive function is found in the normal levels of B12 in TESI+ animals while TESI− animals were deficient. Although the differences in fasting serum gastrin did not approach statistical significance, it is interesting to note that there was a higher trend in TESI− animals, with a known relationship between SBS and elevated gastrin levels.<sup>19</sup> DNA content was higher in TESI than in native intestine after massive small bowel resection and may be accounted for by a thicker muscularis mucosal layer since morphometric measurements of the epithelia were not significantly different between TESI and native intestine.

IAP is a brush border protein which is expressed specifically in differentiated enterocytes, those at the tips of villi, but not by undifferentiated enterocytes or any other cell

type.<sup>20</sup> This makes IAP a useful tool to employ as a marker for differentiation in the intestinal epithelium. The presence of the IAP transcript in the TESI thus indicates that the tissue has undergone, to at least some degree, the process of differentiation. Additionally, the level of the IAP transcript in the TESI+ rats appears more than that in the TESI $\emptyset$  rats. This is of interest as it implies that the TESI, once anastomosed to the resected small bowel (TESI+), possibly undergoes differentiation to a greater degree than the same tissue left implanted in the omentum (TESI $\emptyset$ ). In previous studies,<sup>9–11</sup> an improvement in tissue architecture of tissue engineered stomach, esophagus, colon, and small intestine has been seen with increased length of time from generation and with anastomosis to various locations of the gastrointestinal tract including stomach, small intestine, and colon, implying a role of luminal factors as well as a possible component of maturation over time.

Villin is a calcium-regulated, actin binding protein and is important in the establishment of the apical microvilli in the intestinal brush border, as well as in the brush border of the proximal tubules of the kidneys. Villin mRNA is found in low levels in undifferentiated crypt cells and in higher levels in differentiated villus cells.<sup>21</sup> Its presence in the TESI indicates the presence of a morphology similar to small bowel, a finding which corroborates, at the molecular level, the histologic findings. There appears to be no significant difference in villin mRNA levels between the TESI+ and TESI $\emptyset$ . This is in contrast to our observation with IAP. One possible explanation for this is that both the TESI $\emptyset$  and the TESI+ have established a morphology similar to native small bowel with a crypt-villus axis; however, once the TESI is anastomosed to the resected small bowel (TESI+), it undergoes further differentiation, with an increase in the expression of markers such as IAP. Further analysis of the expression of these and other intestine-specific genes in TESI is required to properly understand the significance of these findings.

Furthermore, GFP labeling demonstrated the donor source of the cells rather than a repopulation of a graft by adjacent tissue, as well as the ease of transfection of the progenitor cells. TESI represents the last, and perhaps most useful, portion of the gastrointestinal tract to be generated using our new protocol with better architecture, present nerve and muscle, and physiologic function. The generation in a similar fashion of tissue-engineered esophagus,<sup>9</sup> stomach,<sup>10</sup> and colon,<sup>8</sup> as well as more specific portions of those tissues,<sup>10</sup> indicates the possibility of very precise intestinal engineering. Adding successful viral transfection opens the possibility of eventual genetic modification of those tissues, for example a tissue-engineered colon expressing SGLT1 or TESI genetically modified to express or overexpress a gene of interest.

We conclude that TESI functions in vivo, meeting basic physiologic demands. We speculate that this technique, if suc-

cessful in higher-order animals, could be a successful way to replace small intestinal function when its lack is a source of morbidity and to avoid the morbidity of treating complications related to other small-intestinal replacement techniques.

## REFERENCES

1. Byrne TA, Nompleggi DJ, Wilmore DW. Advances in the management of patients with intestinal failure. *Trans Proc.* 1996;28:2683–2690.
2. Sundaram A, Koutkia P, Apovian CM. Nutritional management of short bowel syndrome in adults. *J Clin Gastroenterol.* 2002;34:207–220.
3. Stollman NH, Neustater BR, Rogers AI. Short bowel syndrome. *Gastroenterologist.* 1996;4:118–128.
4. Thompson JS. Management of the short bowel syndrome. *Gastroenterol Clin North Am.* 1994;23:403–420.
5. Lykins TC. Comprehensive modified diet simplifies nutrition management. *J Am Diet Assoc.* 1998;98:309–315.
6. Choi RS, Vacanti JP. Preliminary studies of tissue-engineered intestine using isolated epithelial organoid units on tubular synthetic biodegradable scaffolds. *Trans Proc.* 1997;848–851.
7. Evans GS, Flint N, Somers AS, et al. The development of a method for the preparation of rat intestinal epithelial cell primary cultures. *J Cell Sci.* 1992;101:219.
8. Grikscheit T, Ochoa ER, Ramsanahie A, et al. Tissue-engineered large intestine resembles native colon with appropriate in vitro physiology and architecture. *Ann Surg.* 2003;238:35–41.
9. Grikscheit T, Ochoa ER, Srinivasan A, et al. Tissue-engineered esophagus: experimental substitution by onlay patch or interposition. *J Thorac Cardiovasc Surg.* 2003;126:537–544.
10. Grikscheit T, Srinivasan A, Vacanti JP. Tissue-engineered stomach: a preliminary report of a versatile in vivo model with therapeutic potential. *J Pediatr Surg.* 2003;38:1305–1309.
11. Grikscheit TC, Ogilvie JB, Ochoa ER, et al. Tissue engineered colon functions in vivo. *Surgery.* 2002;132:200–204.
12. Choi RS, Pothoulakis C, Kim BS, et al. Studies of brush border enzymes, basement membrane components, and electrophysiology of tissue-engineered neointestine. *J Pediatr Surg.* 1998;33:991–997.
13. Perez A, Grikscheit TC, Blumberg RS, et al. Tissue-engineered small intestine: ontogeny of the immune system. *Transplantation.* 2002;74:619–623.
14. Ramsanahie A, Duxbury M, Grikscheit T, et al. The effect Of GLP-2 on mucosal morphology and SGLT1 expression in tissue engineered neointestine. *Am J Physiol Gastrointest Liver Physiol.* In press.
15. Ory DS, Neugeboren BA, Mulligan RC. A stable human-derived packaging cell line for production of high titer retrovirus/vesicular stomatitis virus G pseudotypes. *Proc Natl Acad Sci USA.* 1996;93:11400–11406.
16. Henthorn PS, Raducha M, Edwards YH, et al. Nucleotide and amino acid sequences of human intestinal alkaline phosphatase: close homology to placental alkaline phosphatase. *Proc Natl Acad Sci USA.* 1987;84:1234–1238.
17. Arpin M, Pringault E, Finidori J, et al. Sequence of human villin: a large duplicated domain homologous with other actin-severing proteins and a unique small carboxy-terminal domain related to villin specificity. *J Cell Biol.* 1993;268:11426–11434.
18. Cleveland DW, Lopata MA, MacDonald RJ, et al. Number and evolutionary conservation of alpha- and beta-tubulin and cytoplasmic beta- and gamma-actin genes using specific cloned cDNA probes. *Cell.* 1980;20:95–105.
19. Nightingale JM, Kamm MA, van der Sijp JR, et al. Gastrointestinal hormones in short bowel syndrome. Peptide YY may be the 'colonic brake' to gastric emptying. *Gut.* 1996;39:267–272.
20. Moog F. Developmental adaptations of alkaline phosphatases in the small intestine. *Fed Proc.* 1962;21:51–56.
21. Robine S, Sahuquillo-Merino C, Louvard D, et al. Regulatory sequences on the human villin gene trigger the expression of a reporter gene in a differentiating HT-29 intestinal cell line. *J Biol Chem.* 1993;268:11426–11434.